Accurate Determination of Human CPR Conformational Equilibrium by smFRET using Dual Orthogonal Non-Canonical Amino Acid Labeling

Robert B. Quast[$], Fataneh Fatemi[†], Michel Kranendonk[⊓], Emmanuel Margeat[‡*], Gilles Truan[$*]

[$]LISBP, Université de Toulouse, CNRS, INRA, INSA, Toulouse, France

[†]Protein Research Center, Shahid Beheshti University, G.C. Evin, Tehran, Iran

[⊓]Center for Toxicogenomics and Human Health (ToxOmics), Genetics, Oncology and Human Toxicology, NOVA Medical School, Faculdade de Ciências Médicas, Universidade Nova de Lisboa, Lisboa, Portugal

[‡]CBS, CNRS, INSERM, Université de Montpellier, Montpellier, France

Corresponding Authors

* Emmanuel Margeat: margeat@cbs.cnrs.fr

* Gilles Truan: gilles.truan@insa-toulouse.fr

ABSTRACT

Conjugation of fluorescent dyes to proteins - a prerequisite for the study of conformational dynamics by single molecule Förster resonance energy transfer (smFRET) – can lead to substantial changes of the dye's photophysical properties, ultimately biasing the quantitative determination of inter-dye distances. In particular the popular cyanine dyes and their derivatives, which are by far the most used dyes in smFRET experiments, exhibit such behavior. To overcome this, a general strategy to site-specifically equip proteins with FRET pairs by chemo-selective reactions using two distinct non-canonical amino acids simultaneously incorporated through genetic code expansion in *Escherichia coli* was developed. Applied to human NADPH-cytochrome P450 reductase (CPR), the importance of homogenously labeled samples for accurate determination of FRET efficiencies was demonstrated. Furthermore, the effect of $NADP^+$ on the ionic strength dependent modulation of the conformational equilibrium of CPR was unveiled. Given its generality and accuracy, the presented methodology establishes a new benchmark to decipher complex molecular dynamics on single molecules.

MAIN TEXT

Numerous biophysical methods can be used to analyze proteins and derive detailed structural information. Albeit their immense power for supporting structural biology, most of these approaches do not resolve the structural dynamics occurring in individual molecules under physiological conditions, a prerequisite for linking conformational information to biochemical function[1]. In particular, conformational transitions may be averaged out using ensemble-based methods, thereby impairing the elucidation of potential short-lived intermediate conformations.

For example, large structural reorientations occurring below the ms timescale have been observed for the human NADPH-cytochrome P450 reductase (CPR) using a variety of different biophysical methods.[2–6] CPR is a paradigmatic diflavin reductase, localized at the endoplasmic reticulum, where it transfers electrons from NADPH to a variety of acceptors including P450 enzymes and plays a major role in essential physiological processes such as drug, steroid and fatty acid metabolism.[7] CPR alternates between a locked, compact state, competent for electron transfer between its two flavin cofactors, bound to distinct FMN and FAD/NADPH domains, and an unlocked, open state, allowing electron transfer to acceptors (Figure 1). In the unlocked state, CPR has been described to experience a large relative conformational freedom of the two flavin binding domains around its flexible hinge segment.[5] The first evidences of these structural rearrangements were provided by crystal structures of a mutant lacking 4 residues in the hinge region[8] and a human:yeast chimera.[9]

Single molecule Förster resonance energy transfer (smFRET) allows for monitoring fast structural changes in proteins by reporting on distances in the range of 2-10 nm

at nanosecond to minute timescales.[1] Nevertheless, smFRET measurements require the site-specific attachment of two organic dyes to the protein-of-interest. The photophysical properties of dyes are sensitive to their physicochemical environment, leading to altered quantum yields (QY) and fluorescence lifetimes,[10] which in turn impact the determination of FRET efficiencies (for details see Supporting Information). However, these parameters can be experimentally determined, allowing for accurate calculation of transfer efficiencies and inter-dye distances provided that only one type of doubly labeled species is present in the sample.[11] In contrast, such a precise correction remains impossible when proteins have been randomly labeled using only one chemical reaction, as each dye will have two different chemical environments affecting its photophysical properties.

Site-specific incorporation of ncAAs into proteins is possible using stop codon suppression mediated by orthogonal translation systems (OTS)[12–15] to provide unique reactive centers for the selective attachment of dyes. Recently, Sadoine et al. labeled calmodulin by a combination of cysteine-maleimide coupling and bioorthogonal reaction of a ncAA to demonstrate the effect of the labeling position on FRET efficiencies.[11] Here, we present a strategy for the accurate assessment of conformational dynamics in proteins by smFRET, exemplified on the soluble form of human CPR. As human CPR contains multiple surface exposed cysteines, one of them being critical for catalysis,[16] we decided to employ a more general labeling strategy comprising two uniquely reactive non-canonical amino acids (ncAAs) followed by subsequent selective fluorescent modification using two bioorthogonal chemistries.

In contrast to previous studies,[14] cotranslational incorporation of *p*-propargyloxy-L-phenylalanine (PrF) and cyclopropene-L-lysine (CpK), mediated by a mutant *M.*

janaschii tyrosyl-tRNA synthetase (PrFRS)/ $tRNA_{CUA}$ pair[17] and the wild type *M. barkeri* pyrrolysyl-tRNA synthetase (CpKRS)/ *M. mazei* $tRNA_{UUA}$, is achieved through parallel suppression of premature *Amber* (TAG/UAG) and *Ochre* (TAA/UAA) stop codons (Figure 2a) using a single newly developed suppression vector. We further measured the influence of the dye position on QYs and demonstrate that our labeling strategy enables accurate determination of FRET efficiencies. Finally, we modulate the conformational dynamics of CPR by salt and confirm the role of the oxidized substrate $NADP^+$ in stabilizing the locked state of CPR.

Based on structures of CPR in a locked (PDB ID 5FA6) and a potential maximally extended state (derived from PDB ID 3FJO, see methods section), surface exposed residues Q160 in the FMN and K671 in the FAD domain were selected for incorporation of ncAAs (Figure 1). Inter-residue distances were estimated to be ~30 Å and ~85 Å for the two conformations, leading to a large FRET efficiency change given the reported Förster radius of 50-55 Å for the Cy3:Cy5 pair.[18] Additionally, T299 served as a constant FRET control in combination with K671, as no change in the inter-residue distance was predicted during the FMN domain movement.

Initial attempts to utilize the previously developed pUltraII system[12] for co-expression of the two OTSs failed to produce soluble sCPR (data not shown). Thus, a novel vector was designed (pRQ101), harboring one cassette for each of the OTSs constructed on the basis of the previously described enhanced pEVOL system.[19] This novel suppression vector allows for an independent induction of the synthetases, thereby enabling a gentle expression of sCPR, obtained through transcriptional leakage of the *lac* promoter in the absence of IPTG. In this way, a set of functional sCPR variants harboring one or both ncAAs at varying positions was produced at yields comparable to previous studies[14] (1-4 mg/ L of purified protein for

double incorporation depending on the position of premature stop codons, (Supplementary Figure S1) and separated from the truncated termination products by two consecutive affinity purifications (Supplementary Figure S2). Although fluorescence modification in a one-pot reaction failed due to unwanted side reactions (Supplementary Figure S3), sequential labeling of CpK by inverse electron-demand Diels-Alder cycloaddition (SPIEDAC) with 6-Methyl-Tetrazine-Sulfo-Cy5 (Cy5-Tet) followed by Copper(II)-dependent azide-alkyne cycloaddition (CuAAC) of PrF with Sulfo-Cy3-Azide (Cy3-N_3) provided perfect specificity (Figure 2b). Furthermore, the degree of labeling of the two fluorophores was calculated around 60% for Cy3 and 90% for Cy5 under optimized conditions (Supplementary Figures S4, S5, S6 and Table S1). The degree of double labeling was thus estimated to be around 50-60% (Supplementary Table S1). Labeled samples of sCPR showed little differences in electron transfer activity (Figure 2c), that were consistent within all doubly labeled constructs and similar to batch-to-batch differences routinely observed between biological replicates.[9,20] Even more importantly, the functional behavior of labeled sCPR variants in response to different NaCl concentrations with a maximal activity at ~500 mM was retained (Figure 2c and Supplementary Figure S7).

The photophysical behavior of the popular cyanine dyes Cy3 and Cy5 is known to be influenced by their local environment.[10] Accordingly, we generated two variants of sCPR in which the positions of donor and acceptor dyes were reversed (Figure 3, $sCPR_{160Cy3,671Cy5}$ and $sCPR_{160Cy5,671Cy3}$) and evaluated the established FRET system by collecting data of freely diffusing single molecules on a homemade confocal setup using alternating pulsed laser excitation (ALEX/PIE).[21]

Distance determination in smFRET experiments depends on the correct determination of the fluorophores quantum yields (Φ_F). Indeed, the D-A distance (R)

is calculated in a FRET experiment using the following equation, where two terms depend on Φ_F:

$$E = \frac{1}{1 + {R^6}/{R_0^6}}$$

Firstly, the Forster radius R_0 depends on the donor QY $\phi_{F,D}$ as follows:

$$R_0 = 0.2108\sqrt[6]{\phi_{F,D}.\kappa^2.n^{-4}.J} \text{ (in Å)}$$

where κ^2 is the orientation factor, n the medium index of refraction and J the spectral overlap integral (in $cm^{-1}.M^{-1}.nm^4$).

Secondly, the transfer efficiency E is measured in a ratiometric smFRET experiment using:

$$E = \frac{I_{FRET}}{\gamma.I_D + I_{FRET}}$$

where I_D and I_{FRET} represent the fluorescence intensities detected for each molecule, i.e. donor and acceptor emissions, respectively (corrected for background and other crosstalk parameters, see Materials and Methods section for details) and where γ represents a correction factor that takes into account the fluorescence QYs of both dyes, and the donor ($G_{G|D}$) and acceptor ($G_{R|A}$) detection efficiencies (which depend on the instrumental characteristics and the emission spectral properties of the fluorophores).

$$\gamma = \frac{G_{R|A}}{G_{G|D}}\frac{\Phi_{F,A}}{\Phi_{F,D}}$$

Thus, any change in the fluorescence QYs (Φ_F) of the dyes needs to be accounted for, to accurately calculate γ, E, R_O and thus R. In this context, it is important to use a homogeneous sample where $\Phi_{F,D}$ and $\Phi_{F,A}$ can be measured for a specific position at which the dye is attached to the protein, a condition that is not fulfilled when using

D-A statistical labeling on two cysteines for example. This requirement is particularly important when using cyanine dyes (such as Cy3, Cy5 and their derivatives), that are widely used in single molecule FRET experiments, and for which local environmental properties lead to strong changes in QYs and fluorescence lifetimes, notably as a consequence of modulation of the rate at which the molecules isomerize from the photo-active trans into the dark cis state[10,22,23].

Often, the apparent FRET efficiency (or proximity ratio) E_{PR} is reported in the literature when only relative distance changes are considered and is calculated without taking into account the γ correction factor:

$$E_{PR} = \frac{I_{FRET}}{I_D + I_{FRET}}$$

Here, comparison of the apparent FRET efficiency $E_{PR(uncorrected)}$ histogram measured for $sCPR_{160Cy3,671Cy5}$ and $sCPR_{160Cy5,671Cy3}$ in the unlocked (open) state, strikingly demonstrated the effect of dye quantum yield changes due to their local environment on the calculation of this parameter (Figure 3). However, thanks to our orthogonal labeling strategy, we generated four singly labeled constructs and calculated the individual, position specific, donor and acceptor quantum yields (Supplementary Table S2). Accounting for these differences, the corrected FRET efficiency distributions turned out to be nearly identical for $sCPR_{160Cy3,671Cy5}$ and $sCPR_{160Cy5,671Cy3}$, underlining the value of the presented approach for acquisition of accurate smFRET data (Figure 3, $E_{corrected}$).

Previous work had shown that the efficiency of cytochrome *c* reduction by sCPR is directly related to the conformational equilibrium, which can be modulated by ionic strength.[3,5] Accordingly, the FRET efficiencies of the $sCPR_{160Cy3,671Cy5}$ variant decreased with increasing concentrations of NaCl (Figure 4a). This corresponds to an increase of the average inter-dye distance and thus a shift of the equilibrium in

favor of the unlocked state. We validated this interpretation using two constructs: first, the $sCPR_{160Cy5,671Cy3}$, for which the two dyes are inverted, displayed a similar salt-dependent shift of the FRET distribution as expected (data not shown). Second, the aforementioned $sCPR_{299Cy3,671Cy5}$ variant showed no inter-dye distance changes in response to ionic strength variations (Supplementary Table S3 and Figure S8).

We noted that in all cases, the width of the FRET efficiency distributions were wider than what would be predicted for a single donor-acceptor distance, taking into account the distribution broadening due to photon shot noise. This effect is particularly visible at conditions above physiological ionic strength (≥500 mM), and could point to the presence of multiple conformations in the unlocked state, interconverting in the ms timescale, in accordance with previous SAXS, NMR[5] and smFRET data.[24]

Several studies have provided evidence for a closing of sCPR induced by its oxidized substrate $NADP^+$.[2,25,26] For comparison we fitted the smFRET data obtained in the presence and absence of 500 µM $NADP^+$ to a previously developed salt-dependent two state model of the conformational equilibrium.[5] In the presence of $NADP^+$ a shift of the mid-point transition to higher NaCl was observed (Figure 4b). However, the overall distribution of FRET efficiencies remained strikingly similar when compared to data obtained in the absence of $NADP^+$ (Figure 4c). Notably, a maximal average distance of 57 Å of the two dyes was calculated in the unlocked state at 1 M NaCl, which was only slightly reduced to 53 Å when $NADP^+$ was present. Altogether, $NADP^+$ binding seems not to be sufficient to close the sCPR structure per se, but rather shifts the mid-point of the conformational equilibrium to stabilize the locked state and has no general effect on the distribution of potential conformational subpopulations. Physiologically, the ionic strength is equivalent to

about 170 mM NaCl, and the reported $NADP^+$ concentration is around 5 μM (100 times lower than the one we used). [27] We can thus hypothesize that the shift in the equilibrium induced by the oxidized cofactor on oxidized CPR is probably minor under physiological conditions.

In this study, we presented a general strategy for the domain-selective equipment of human CPR with a FRET pair to enable an accurate single molecule analysis of conformational dynamics. The developed labeling strategy is of high value for attachment of dyes to any protein for which cysteine and other labeling strategies are inapplicable. It is easily adaptable for the study of diverse biological questions because i) the used OTSs, ncAAs and the FRET pair are easily accessible from academic laboratories and/or commercial sources, ii) they are interchangeable allowing for free choice of ncAAs, labeling reactions and FRET pair, iii) only a single suppression vector has to be co-transformed together with the expression vector for the protein-of-interest and iv) the parallel suppression of two stop codons eliminates the need for any additional components to facilitate efficient ncAA incorporation with high fidelity.

Although a variety of biophysical methods have been applied to study the domain movements in CPR,[2,4,5,25,26,28,29] the newly established FRET system offers a valuable complementation as it enables studying single molecules at timescales inaccessible by other methods within complex biological environments. With the fast pace of technical and methodological advances we envision that this system will provide new insights into the structural dynamics of CPR as a prototypical diflavin reductase but also help to assess, with a very high precision, the potential roles of cofactors binding on the structural transitions. As such, CPR can be considered as a model for multidomain proteins exhibiting large and fast conformational transitions.

ASSOCIATED CONTENT

A detailed experimental description of template generation, protein expression, protein purification, protein labeling, cytochrome c reduction assay, quantum yield determination, smFRET measurements and data analysis, modeling of CPR open conformation, curve fitting, calculation of Förster radius and total distances, supplementary figures, supplementary tables and gene and protein sequences is available in the supplementary material.

ACKNOWLEDGMENTS

This work was in part funded by a joint ANR/FCT program; France: ANR-13-ISV5-0001 (DODYCOEL), and Portuguese national funds, through the Fundação para a Ciência e a Tecnologia (Project FCT-ANR/BEX-BCM/0002/2013). The CBS belongs to the France-BioImaging infrastructure supported by the French National Research Agency (ANR-10-INBS-04, "Investments for the future"), and is supported by the GIS "IBiSA: Infrastructures en Biologie Sante et Agronomie". Additonally, RBQ was supported by an "Access grant" from the France-BioImaging infrastructure. We thank the committee of the INSEERE project, in particular Régis Faure, Sébastien Nouaille and Virginie Ramillon-Delvolve for assistance in molecular biology and Hélène Cordier for access to the Biorad Imaging System. Further we thank Philippe Urban for critical reading of the manuscript.

COMPETING INTERESTS

The authors declare no competing interests.

REFERENCES

(1) Lerner, E.; Cordes, T.; Ingargiola, A.; Alhadid, Y.; Chung, S.; Michalet, X.; Weiss, S. Toward Dynamic Structural Biology: Two Decades of Single-Molecule Förster Resonance Energy Transfer. *Science* **2018**, *359* (6373), eaan1133.

(2) Pudney, C. R.; Khara, B.; Johannissen, L. O.; Scrutton, N. S. Coupled Motions Direct Electrons along Human Microsomal P450 Chains. *PLoS Biol.* **2011**, *9* (12), e1001222.

(3) Huang, W.-C.; Ellis, J.; Moody, P. C. E.; Raven, E. L.; Roberts, G. C. K. Redox-Linked Domain Movements in the Catalytic Cycle of Cytochrome P450 Reductase. *Structure* **2013**, *21* (9), 1581–1589.

(4) Laursen, T.; Singha, A.; Rantzau, N.; Tutkus, M.; Borch, J.; Hedegård, P.; Stamou, D.; Møller, B. L.; Hatzakis, N. S. Single Molecule Activity Measurements of Cytochrome P450 Oxidoreductase Reveal the Existence of Two Discrete Functional States. *ACS Chem. Biol.* **2014**, *9* (3), 630–634.

(5) Frances, O.; Fatemi, F.; Pompon, D.; Guittet, E.; Sizun, C.; Pérez, J.; Lescop, E.; Truan, G. A Well-Balanced Preexisting Equilibrium Governs Electron Flux Efficiency of a Multidomain Diflavin Reductase. *Biophys. J.* **2015**, *108* (6), 1527–1536.

(6) Kovrigina, E. A.; Pattengale, B.; Xia, C.; Galiakhmetov, A. R.; Huang, J.; Kim, J.-J. P.; Kovrigin, E. L. Conformational States of Cytochrome P450 Oxidoreductase Evaluated by Förster Resonance Energy Transfer Using Ultrafast Transient Absorption Spectroscopy. *Biochemistry* **2016**, *55* (43), 5973–5976.

(7) Riddick, D. S.; Ding, X.; Wolf, C. R.; Porter, T. D.; Pandey, A. V.; Zhang, Q.-Y.; Gu, J.; Finn, R. D.; Ronseaux, S.; McLaughlin, L. A.; et al. NADPH–Cytochrome P450 Oxidoreductase: Roles in Physiology, Pharmacology, and Toxicology. *Drug*

Metab. Dispos. **2013**, *41* (1), 12–23.

(8) Hamdane, D.; Xia, C.; Im, S.-C.; Zhang, H.; Kim, J.-J. P.; Waskell, L. Structure and Function of an NADPH-Cytochrome P450 Oxidoreductase in an Open Conformation Capable of Reducing Cytochrome P450. *J. Biol. Chem.* **2009**, *284* (17), 11374–11384.

(9) Aigrain, L.; Pompon, D.; Moréra, S.; Truan, G. Structure of the Open Conformation of a Functional Chimeric NADPH Cytochrome P450 Reductase. *EMBO Rep.* **2009**, *10* (7), 742–747.

(10) Aramendia, P. F.; Negri, R. M.; Roman, E. S. Temperature Dependence of Fluorescence and Photoisomerization in Symmetric Carbocyanines.Influence of Medium Viscosity and Molecular Structure. *J. Phys. Chem.* **1994**, *98* (12), 3165–3173.

(11) Sadoine, M.; Cerminara, M.; Kempf, N.; Gerrits, M.; Fitter, J.; Katranidis, A. Selective Double-Labeling of Cell-Free Synthesized Proteins for More Accurate smFRET Studies. *Anal. Chem.* **2017**, *89* (21), 11278–11285.

(12) Chatterjee, A.; Sun, S. B.; Furman, J. L.; Xiao, H.; Schultz, P. G. A Versatile Platform for Single- and Multiple-Unnatural Amino Acid Mutagenesis in Escherichia coli. *Biochemistry* **2013**, *52* (10), 1828–1837.

(13) Kim, J.; Seo, M.-H.; Lee, S.; Cho, K.; Yang, A.; Woo, K.; Kim, H.-S.; Park, H.-S. Simple and Efficient Strategy for Site-Specific Dual Labeling of Proteins for Single-Molecule Fluorescence Resonance Energy Transfer Analysis. *Anal. Chem.* **2013**, *85* (3), 1468–1474.

(14) Sachdeva, A.; Wang, K.; Elliott, T.; Chin, J. W. Concerted, Rapid, Quantitative, and Site-Specific Dual Labeling of Proteins. *J. Am. Chem. Soc.* **2014**, *136* (22), 7785–7788.

(15) Wang, K.; Sachdeva, A.; Cox, D. J.; Wilf, N. M.; Lang, K.; Wallace, S.; Mehl, R. A.; Chin, J. W. Optimized Orthogonal Translation of Unnatural Amino Acids Enables Spontaneous Protein Double-Labelling and FRET. *Nat. Chem.* **2014**, *6* (5), 393–403.

(16) Shen, A. L.; Christensen, M. J.; Kasper, C. B. NADPH-Cytochrome P-450 Oxidoreductase. The Role of Cysteine 566 in Catalysis and Cofactor Binding. *J. Biol. Chem.* **1991**, *266* (30), 19976–19980.

(17) Deiters, A.; Schultz, P. G. In Vivo Incorporation of an Alkyne into Proteins in Escherichia coli. *Bioorg. Med. Chem. Lett.* **2005**, *15* (5), 1521–1524.

(18) Dietrich, A.; Buschmann, V.; Müller, C.; Sauer, M. Fluorescence Resonance Energy Transfer (FRET) and Competing Processes in Donor-Acceptor Substituted DNA Strands: A Comparative Study of Ensemble and Single-Molecule Data. *J. Biotechnol.* **2002**, *82* (3), 211–231.

(19) Young, T. S.; Ahmad, I.; Yin, J. A.; Schultz, P. G. An Enhanced System for Unnatural Amino Acid Mutagenesis in E. coli. *J. Mol. Biol.* **2010**, *395* (2), 361–374.

(20) Campelo, D.; Lautier, T.; Urban, P.; Esteves, F.; Bozonnet, S.; Truan, G.; Kranendonk, M. The Hinge Segment of Human NADPH-Cytochrome P450 Reductase in Conformational Switching: The Critical Role of Ionic Strength. *Front. Pharmacol.* **2017**, *8*.

(21) Olofsson, L.; Margeat, E. Pulsed Interleaved Excitation Fluorescence Spectroscopy with a Supercontinuum Source. *Opt. Express* **2013**, *21* (3), 3370–3378.

(22) Sanborn, M. E.; Connolly, B. K.; Gurunathan, K.; Levitus, M. Fluorescence Properties and Photophysics of the Sulfoindocyanine Cy3 Linked Covalently to DNA. *J. Phys. Chem. B* **2007**, *111* (37), 11064–11074.

(23) Berlier, J. E.; Rothe, A.; Buller, G.; Bradford, J.; Gray, D. R.; Filanoski, B. J.; Telford, W. G.; Yue, S.; Liu, J.; Cheung, C.-Y.; et al. Quantitative Comparison of Long-Wavelength Alexa Fluor Dyes to Cy Dyes: Fluorescence of the Dyes and Their Bioconjugates. *J. Histochem. Cytochem. Off. J. Histochem. Soc.* **2003**, *51* (12), 1699–1712.

(24) Bavishi, K.; Li, D.; Eiersholt, S.; Hooley, E. N.; Petersen, T. C.; Møller, B. L.; Hatzakis, N. S.; Laursen, T. Direct Observation of Multiple Conformational States in Cytochrome P450 Oxidoreductase and Their Modulation by Membrane Environment and Ionic Strength. *Sci. Rep.* **2018**, *8* (1).

(25) Ellis, J.; Gutierrez, A.; Barsukov, I. L.; Huang, W.-C.; Grossmann, J. G.; Roberts, G. C. K. Domain Motion in Cytochrome P450 Reductase: Conformational Equilibria Revealed by NMR and Small-Angle X-Ray Scattering. *J. Biol. Chem.* **2009**, *284* (52), 36628–36637.

(26) Wadsater, M.; Laursen, T.; Singha, A.; Hatzakis, N. S.; Stamou, D.; Barker, R.; Mortensen, K.; Feidenhans'l, R.; Lindberg Moller, B.; Cardenas, M. Monitoring Shifts in the Conformation Equilibrium of the Membrane Protein Cytochrome P450 Reductase (POR) in Nanodiscs. *J. Biol. Chem.* **2012**.

(27) Lu, W.; Wang, L.; Chen, L.; Hui, S.; Rabinowitz, J. D. Extraction and Quantitation of Nicotinamide Adenine Dinucleotide Redox Cofactors. *Antioxid. Redox Signal.* **2018**, *28* (3), 167–179.

(28) Hedison, T. M.; Hay, S.; Scrutton, N. S. Real-Time Analysis of Conformational Control in Electron Transfer Reactions of Human Cytochrome P450 Reductase with Cytochrome c. *FEBS J.* **2015**, *282* (22), 4357–4375.

(29) Hay, S.; Brenner, S.; Khara, B.; Quinn, A. M.; Rigby, S. E. J.; Scrutton, N. S. Nature of the Energy Landscape for Gated Electron Transfer in a Dynamic Redox

Protein. *J. Am. Chem. Soc.* **2010**, *132* (28), 9738–9745.

FIGURES

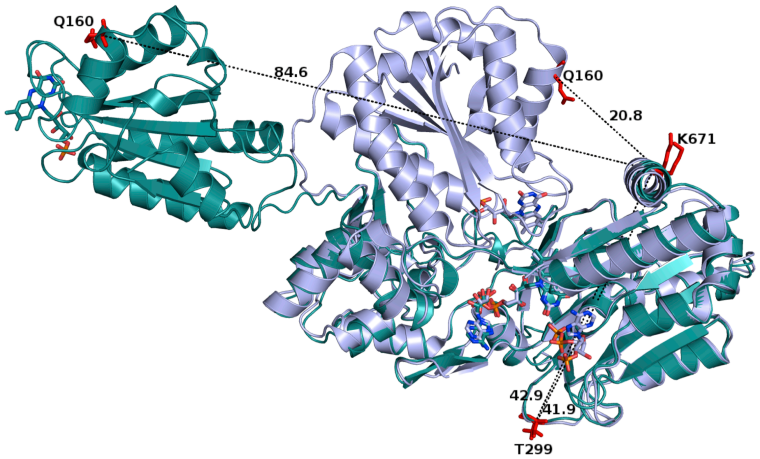

Figure 1. Overlay of compact (grey, PDB code 5FA6) and extended (green, human extended conformation model based on 3FJO) conformations of soluble human CPR with highlighted distances (Å) of residues selected for installation of fluorescent moieties (red). The FMN, FAD and $NADP^+$ molecules are shown as sticks.

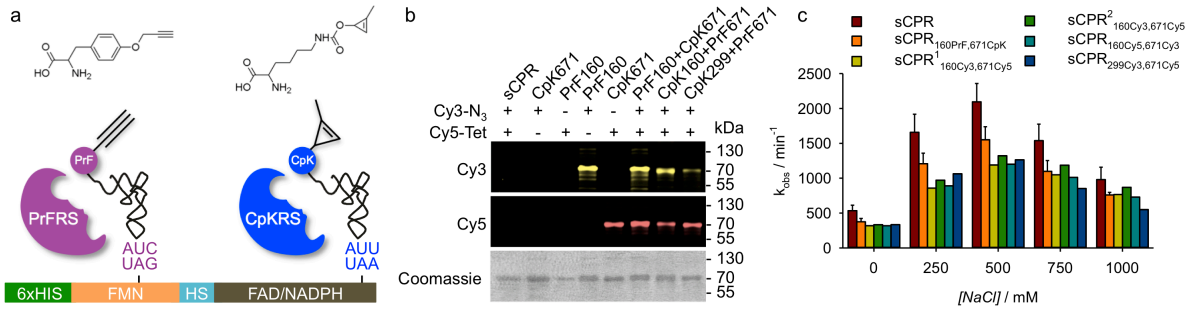

Figure 2. Cotranslational incorporation of ncAAs and chemoselective fluorescence modification. a) Parallel incorporation of PrF (left) by *Amber* (purple) and CpK (right) by *Ochre* (blue) suppression mediated by PrFRS/tRNA$_{CUA}$ and CpKRS/tRNA$_{UUA}$, respectively. The schematic representation of the sCPR gene includes the N-terminal 6 x Histidine tag (green), the FMN domain (yellow), the hinge segment (HS, cyan) and the FAD/NADPH domain (brown). b) Bioorthogonal modification of incorporated PrF with Sulfo-Cy3-Azide (Cy3-N3) by CuAAC and CpK with Tetrazine-Sulfo-Cy5 (Cy5-Tet) by SPIEDAC. c) Cytochrome *c* reduction efficiency of labeled sCPR variants given by the initial velocity k_{obs}. Error bars represent the standard deviation of triplicates. For sCPR$_{160Cy3,671Cy5}$ data is shown for individual samples later used in smFRET measurements.

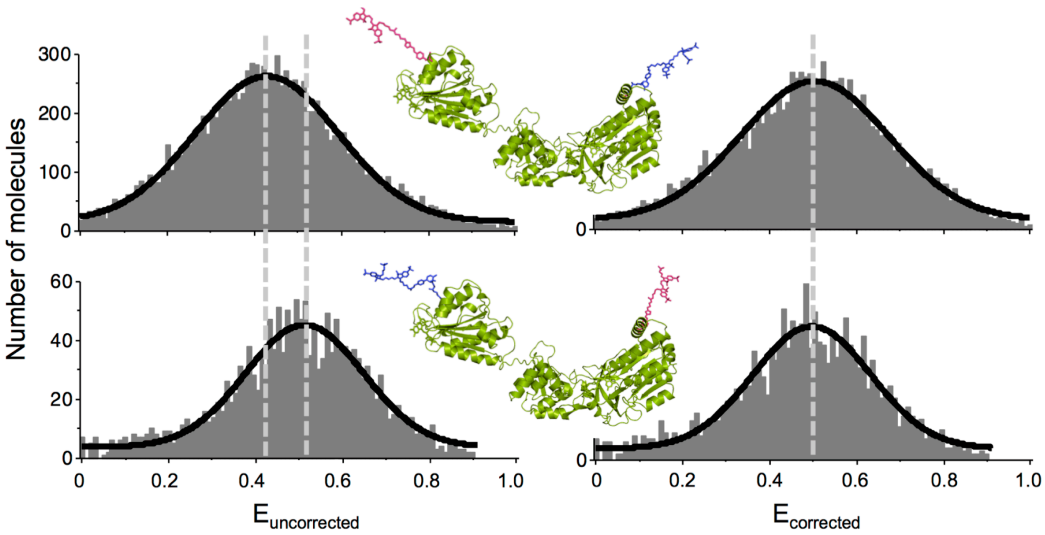

Figure 3. Influence of labeling position on FRET efficiency. Uncorrected (left) and QY corrected (center) histograms of sCPR labeled with Cy3 (magenta) on FMN and Cy5 (blue) on FAD domain ($sCPR_{160Cy3,671Cy5}$, top) and vice versa ($sCPR_{160Cy5,671Cy3}$, bottom). Dashed lines indicate peak positions.

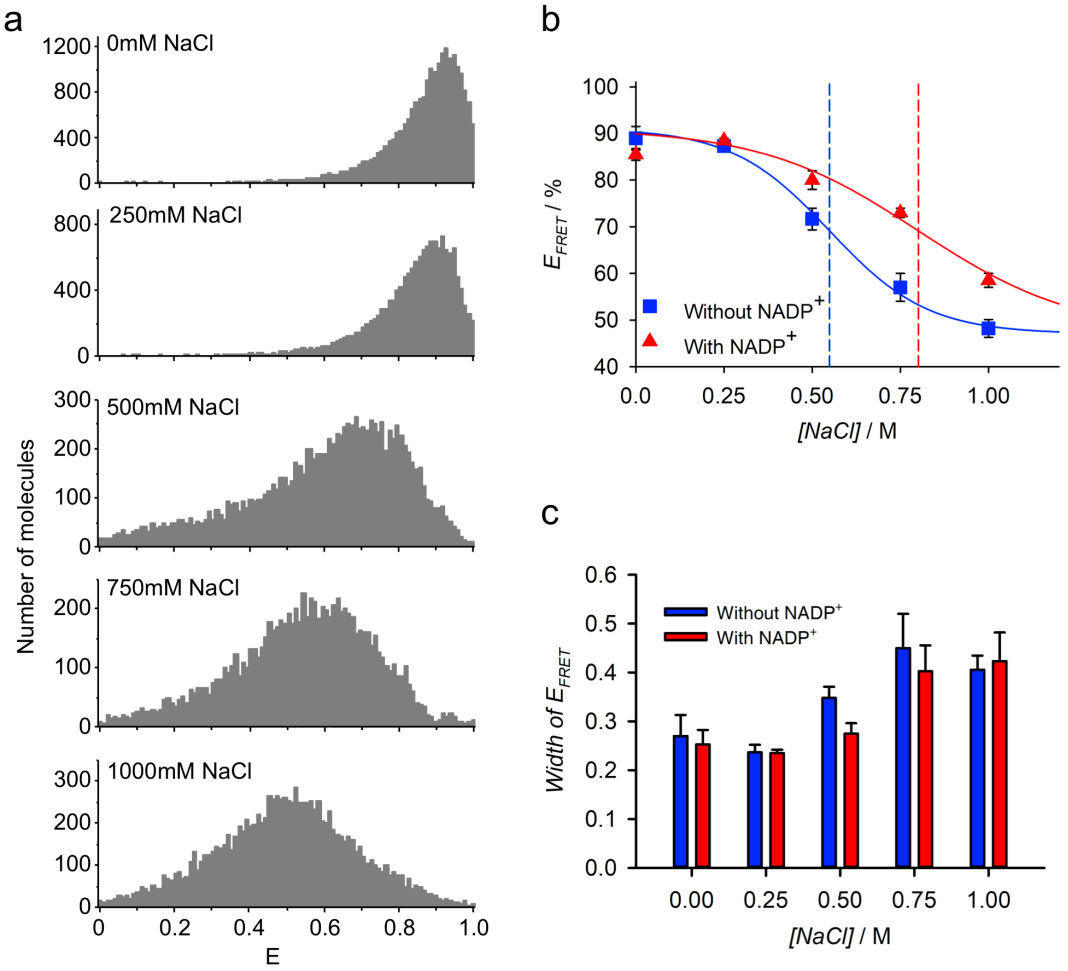

Figure 4. Ionic strength dependent modulation of conformational equilibrium between locked and unlocked states. a) FRET efficiency histograms of $sCPR_{160Cy3,671Cy5}$ at different NaCl concentrations. b) Influence of $NADP^+$ on equilibrium. Data points represent maxima of the FRET efficiency in the absence (blue squares) and presence (red triangles) of 500 µM $NADP^+$. Functions were derived by fitting a two state model (see text) and the mid-point transition is indicated by a dashed line. c) Widths of FRET efficiency distributions fitted by a Gaussian function, at different NaCl concentrations.